11th World Congress on Computational Mechanics (WCCM XI)
5th European Conference on Computational Mechanics (ECCM V)
6th European Conference on Computational Fluid Dynamics (ECFD VI)
E. Oñate, J. Oliver and A. Huerta (Eds)

NUMERICAL VALIDATION OF A κ-ω-κ_θ-ω_θ HEAT TRANSFER TURBULENCE MODEL FOR LOW PRANDTL NUMBER FLUIDS.

D. Cerroni, S. Manservisi and F. Menghini[1]

DIN - Laboratory of Montecuccolino, Via dei Colli, 16, 40136 Bologna, Italy.
[1] filippo.menghini3@unibo.it

Key words: Turbulence model, Heat transfer correlations, Heavy liquid metal

Abstract. In ordinary fluids with $Pr \sim 1$ it is well known that a two equation turbulence model with a constant turbulent Prandtl number $Pr_t \sim 0.85$ is usually sufficient to correctly predict heat transfer in fully turbulent flows. On the contrary, in heavy liquid metals the simple hypothesis of constant Pr_t cannot reproduce experimental data and the turbulent Prandtl number Pr_t has to be introduced as a function of state variables. In this work we introduce a four parameter turbulence model that may improve heat transfer prediction in fully developed heavy liquid metal flows. The turbulent heat flux transport equation is solved algebraically and an expression for the thermal eddy diffusivity α_t is obtained. This quantity depends on the thermal and dynamical time scales of turbulence and their ratio. A four parameter turbulence model κ-ϵ-κ_θ-ϵ_θ for low-Prandtl number fluids has been already presented by the authors with satisfactory results. The main problem of the κ-ϵ models is the stability of the system since ϵ is a function of κ on the boundary. The introduction of the κ-ω system allows to calculate directly the time scale of turbulence as $\tau = \omega^{-1}$ and to achieve a more stable and robust solution near the wall. Numerical results are obtained by using an in-house code with a standard finite element implementation of Navier-Stokes equations coupled with the four parameter turbulence model. The code allows multiple refinement of the mesh in order to improve the solution and to correctly impose the boundary conditions with a near-wall approach. Results from simulations of fully developed turbulent flows of heavy liquid metals are reported for the plane and cylindrical geometries, in particular for the heat transfer between a wall heated with uniform heat flux and the liquid metal flow. The results are compared with DNS data when available and with experimental heat transfer correlations for the prediction of the Nusselt number in order to evaluate the turbulence model.

1 INTRODUCTION

Heavy liquid metals are studied from several years by the engineering community, since these fluids are considered as coolants for fast nuclear reactors, in order to achieve the necessary requirements for the Generation IV nuclear reactors. These fluids show a peculiar heat transfer and fluid-dynamic properties because of their very high conductivity and low viscosity. For these characteristic physical properties heavy liquid metals are often referred to as Low-Prandtl number fluids. Despite their several advantages, these fluids are not well known as ordinary fluids because experiments carried on them are very challenging and the corresponding experimental errors very high [1]. A very deep knowledge of heat transfer and fluid flow properties can be achieved with Direct Numerical Simulation (DNS). With DNS the profiles of velocity, temperature and other turbulent quantities can be obtained, but unfortunately this is possible only for flows with very low Reynolds numbers and in very simple geometries because of the high computational cost which is required by DNS computations. For these reasons in the last years many projects have been started with the purpose of developing turbulence models and Computational Fluid Dynamics (CFD) codes able to correctly predict heat transfer in fully developed heavy liquid metal turbulent flows with a not too high computational cost.

It has been proved by many studies that, for liquid metal flows, turbulence models based on a constant turbulent Prandtl number fail to reproduce the available experimental heat transfer correlations, see for instance [1, 2]. An hypothesis of a constant turbulent Prandtl number implies that the thermal eddy diffusivity is simply proportional to the momentum eddy diffusivity and this is commonly implemented in commercial codes. Such a turbulence model is referred to as Simple Eddy Diffusivity, SED. In Figure 1 on the left

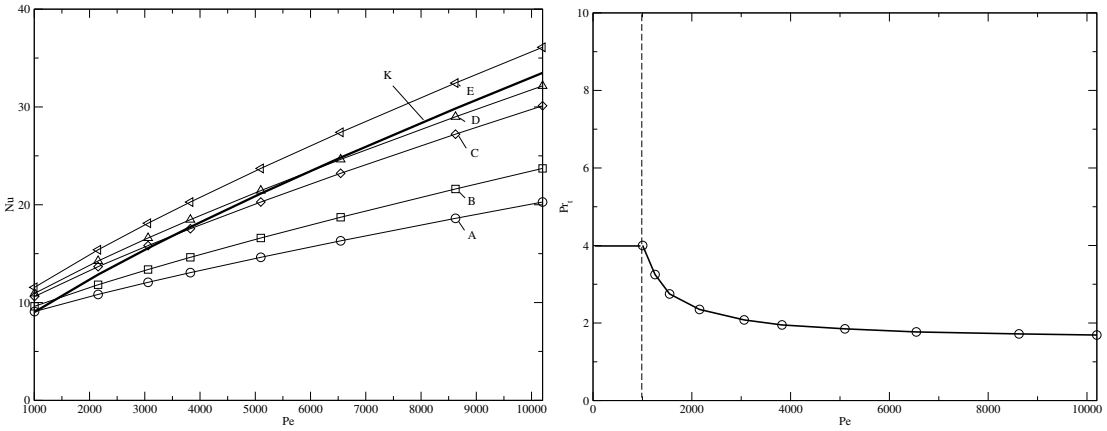

Figure 1: Asymptotic Nusselt number Nu as a function of the Peclet number Pe for the cylinder channel heated with constant heat flux (left): numerical results obtained with the SED model implemented in Fluent with $Pr_t = 4$(A), 3(B), 2(C), 1.8(D) and 1.5(E) compared with the empirical Kirillov-Ushakov correlation (K). Values of the turbulent Prandtl number necessary to match experimental correlations by Kirillov-Ushakov as a function of the Peclet number Pe (right).

the asymptotic Nusselt number for a fully developed heavy liquid metal flow in a simple rod heated with constant heat flux is reported. Results obtained with the SED model implemented in Fluent with constant turbulent Prandtl number $Pr_t = 4$ (A), 3 (B), 2 (C), 1.8 (D) and 1.5 (E) are compared with Kirillov-Ushakov heat transfer correlation for the same geometrical configuration. This correlation reads [5]

$$Nu = 4.5 + 0.018\, Pe^{0.8} \quad 10^4 \leq Re \leq 5 \cdot 10^6\,. \tag{1}$$

It can be easily seen from this Figure that a SED model with constant turbulent Prandtl number cannot reproduce the experimental results. If Pr_t is set as a function of Peclet number as reported in Figure 1 on the right, then a good match with experimental results can be obtained. Unfortunately a different function for Pr_t has to be found for any different geometry and boundary condition configuration, so it is rather complicated to correctly predict heat transfer in complex geometries.

A different approach to the problem is to solve the transport equation for the turbulent heat flux. Algebraic solutions of this equation can be obtained using temperature and velocity time scales of turbulence [6]. By solving this equation with explicit methods one may obtain an expression for the thermal eddy diffusivity, defined as the ratio between the turbulent heat flux and the temperature gradient. In order to obtain the turbulent heat flux with these methods two additional transport equations must be solved for the mean square temperature fluctuation κ_θ and its dissipation. In this work we propose a four parameter heat transfer turbulence model based on κ-ω Shear-Stress Transport model and on κ_θ-ω_θ model obtained from the κ_θ-ϵ_θ model proposed in [3, 4]. The use of κ-ω models results in a much more robust numerical implementation.

In the next section we introduce heat and momentum transport equations which includes Navier-Stokes equations, κ-ω SST turbulence equations and κ_θ-ω_θ equations for the turbulent heat transfer model. The definition of the thermal eddy diffusivity with the model functions used is explained in details. In the third section we report the preliminary numerical results obtained with this turbulence model for two geometrical configurations, plane and cylindrical channel. We compare plane results at low Reynolds numbers with DNS data and cylindrical results with experimental heat transfer correlations. Finally conclusions are taken over the validity of this model and the improvements obtained with respect to κ_θ-ϵ_θ model as reported in [3].

2 HEAT AND MOMENTUM TRANSPORT EQUATIONS

Heavy liquid metals can be considered as incompressible fluids in most of the practical applications where they are employed. The fluid motion and heat transfer are based on Navier-Stokes and energy balance equations. Reynolds averaging procedure can be applied to the fundamental transport equations in order to obtain a system for averaged fields $(\vec{u}, p, T)$. Once the Reynolds averaging procedure is carried on the system one gets

is

$$\frac{\partial u_k}{\partial x_k} = 0\,, \tag{2}$$

$$\rho\frac{\partial u_i}{\partial t} + \rho u_k\frac{\partial u_i}{\partial x_k} = \frac{\partial}{\partial x_j}\sigma_{ij} - \frac{\partial}{\partial x_k}\rho\overline{u_k' u_i'} + \rho g_i\,, \tag{3}$$

$$\rho C_p\left(\frac{\partial T}{\partial t} + u_k\frac{\partial T}{\partial x_k}\right) = \frac{\partial}{\partial x_k}\left(\lambda\frac{\partial T}{\partial x_k}\right) - \frac{\partial}{\partial x_k}\rho C_p\overline{u_k' T'} + Q\,, \tag{4}$$

where $\vec{u}$ and T are the average velocity and temperature fields. By applying Reynolds averaging procedure two new variables appear which take into account the effect of turbulence: the Reynolds stress tensor $\rho\overline{u_k' u_i'}$, which is the average product of velocity fluctuations and the turbulent heat flux vector $\rho C_p\overline{u_k' T'}$, which is the average product of velocity and temperature fluctuations. From Navier-Stokes system we can define the stress tensor σ_{ij} and the velocity deformation tensor S_{ij} as

$$\sigma_{ij} = -p\delta_{ij} + \mu S_{ij} \qquad S_{ij} = \frac{\partial u_i}{\partial x_j} + \frac{\partial u_j}{\partial x_i}\,, \tag{5}$$

where μ is the molecular viscosity and p the average static pressure. The system (2-4) is not close unless the Reynolds stress tensor and the turbulent heat flux are defined. These unknowns could be obtained as solutions of two transport equations: the Reynolds stress transport equation and the turbulent heat flux transport equation. However, direct solutions of these equations are difficult to obtain. Instead, usually one uses the concept of momentum and thermal eddy diffusivity and the Reynolds stress and the turbulent heat flux are modeled.

For general flow situations the momentum eddy diffusivity model may be written as

$$\overline{u_i' u_j'} = -\nu_t\left(\frac{\partial u_i}{\partial x_j} + \frac{\partial u_j}{\partial x_i}\right) + \frac{2\kappa}{3}\,\delta_{ij}\,, \tag{6}$$

where κ and ν_t are the turbulent kinetic energy and the momentum eddy diffusivity, respectively. The last term in (6) assures that the sum of the normal stresses is equal to 2κ, which is required by the definition of κ. The normal stresses act like pressure forces, so they can be absorbed into the pressure-gradient term and the static pressure is replaced as an unknown quantity by the modified pressure. One of the most popular model to compute the turbulent viscosity ν_t is

$$\nu_t = C_\mu\,\kappa\tau_u \tag{7}$$

where $C_\mu = 0.09$ and τ_u is the local dynamical characteristic time. The local dynamical characteristic time can be computed directly if one uses κ-ω turbulence models as

$$\tau_u = \frac{1}{\omega}\,. \tag{8}$$

In the SST model the local dynamical time is defined as the minimum between the time usually defined in κ-ω turbulence models and a local time based on the deformation tensor S in this way [10]:

$$\tau_u = \min\left\{\frac{1}{\omega}\,,\,\frac{0.31}{SF_2}\right\}\,, \tag{9}$$

where F_2 is a model variable defined in the following. The turbulent kinetic energy κ, its dissipation ϵ and the specific dissipation rate ω are defined by

$$\kappa = \frac{1}{2}\overline{u_i' u_i'} \qquad \epsilon = \nu\overline{\left(\frac{\partial u_i'}{\partial x_j}\right)\left(\frac{\partial u_i'}{\partial x_j}\right)}\,, \qquad \omega = \frac{\epsilon}{C_\mu\,\kappa}\,. \tag{10}$$

The equation for κ can be written in the following form

$$\frac{\partial \kappa}{\partial t} + u_i\frac{\partial \kappa}{\partial x_i} = \frac{\partial}{\partial x_j}\left[\left(\nu + \frac{\nu_t}{\sigma_\kappa}\right)\frac{\partial \kappa}{\partial x_j}\right] + P_\kappa - C_\mu\omega\kappa\,. \tag{11}$$

with

$$P_\kappa = -\overline{u_i' u_j'}\,\frac{\partial u_i}{\partial x_j} = \nu_t\left(\frac{\partial u_i}{\partial x_j} + \frac{\partial u_j}{\partial x_i}\right)\frac{\partial u_i}{\partial x_j}\,. \tag{12}$$

In the SST model the production term of κ is limited with a maximum value of ten times the dissipation term, namely $10\,C_\mu\omega\kappa$. The equation for ω in the SST model is written as [10]

$$\frac{\partial \omega}{\partial t} + u_i\frac{\partial \omega}{\partial x_i} = \frac{\partial}{\partial x_j}\left[\left(\nu + \frac{\nu_t}{\sigma_\omega}\right)\frac{\partial \omega}{\partial x_j}\right] + \alpha S^2 - \beta\omega^2 + \frac{2(1-F_1)}{\omega}\frac{\partial \kappa}{\partial x_j}\frac{\partial \omega}{\partial x_j}\,. \tag{13}$$

In SST model all the variables σ_κ, σ_ω, α and β are defined as functions of the variable F_1 in order to get a good switch between the κ-ϵ and the κ-ω models in the regions where they are more appropriate to use, near wall for κ-ω and center of the channel for κ-ϵ. The variable F_1 is defined as

$$F_1 = \tanh\left\{\left\{\min\left[\max\left(\frac{\sqrt{\kappa}}{C_\mu\omega d}\,,\,\frac{500\nu}{\omega d^2}\right)\,,\,\frac{3.424\kappa}{CD_{\kappa\omega}d^2}\right]\right\}^4\right\}\,, \tag{14}$$

with d the distance from the wall and

$$CD_{\kappa\omega} = \max\left(\frac{1.712\rho}{\omega}\frac{\partial \kappa}{\partial x_j}\frac{\partial \omega}{\partial x_j}\,,\,10^{-10}\right)\,. \tag{15}$$

σ_κ, σ_ω, α and β are defined basing on F_1 as

$$\begin{aligned}
\sigma_\kappa &= 0.85 + (1 - F_1)\\
\sigma_\omega &= 0.5 + 0.856(1 - F_1)\\
\alpha &= \frac{5}{9} + 0.44(1 - F_1)\\
\beta &= \frac{3}{40} + 0.0828(1 - F_1)\,.
\end{aligned}$$

Finally, the variable F_2 is used for the calculation of the momentum eddy diffusivity and is defined as

$$F_2 = \tanh\left\{\left[\max\left(\frac{2\sqrt{\kappa}}{C_\mu \omega d}\,,\,\frac{500\nu}{\omega d^2}\right)\right]^2\right\}. \tag{16}$$

In a similar way as we did for the Reynolds stress tensor we can solve the turbulent heat flux transport equation with an approximate algebraic solution [6]. For the turbulent heat flux transport equation we may approximate the solution as

$$\overline{u_i' T'} \;=\; -\alpha_t \left(\frac{\partial T}{\partial x_i}\right)\;, \tag{17}$$

where α_t is the thermal eddy diffusivity. In analogy with the dynamical case the thermal diffusivity α_t may be defined as

$$\alpha_t = C_\theta\, \kappa \tau_{l\theta}\,, \tag{18}$$

where $C_\theta = 0.1 = C_\mu/0.9$ and $\tau_{l\theta}$ is the local thermal characteristic time that takes into account the corrections near the wall region. In analogy with the definitions in (10) we introduce the average square temperature fluctuation κ_θ, its dissipation ϵ_θ and its specific dissipation rate ω_θ as

$$\kappa_\theta = \frac{1}{2}\overline{T'^2}\,, \qquad \epsilon_\theta = \frac{\nu}{Pr}\overline{\left(\frac{\partial T'}{\partial x_i}\right)\left(\frac{\partial T'}{\partial x_i}\right)} \qquad \omega_\theta = \frac{\epsilon_\theta}{C_\mu \kappa_\theta} \tag{19}$$

and define the characteristic time $\tau_\theta = 1/\omega_\theta$ and the ratio $R = \tau_\theta/\tau_u = \omega/\omega_\theta$ between the thermal turbulent characteristic time and the dynamical turbulent characteristic time. The local thermal characteristic time $\tau_{l\theta}$ can be modeled with the introduction of the proper thermal characteristic time $\tau_\theta = 1/\omega_\theta$ as

$$\tau_{l\theta} = \Big(f_{1\theta}\, B_{1\theta} + f_{2\theta}\, B_{2\theta}\Big)\,, \tag{20}$$

whit $f_{1\theta}$, $B_{1\theta}$, $f_{2\theta}$ and $B_{2\theta}$ are appropriate functions. We set

$$f_{1\theta} = (1 - \exp(-0.0526\,\frac{R_\delta}{\sqrt{Pr}}))\,(1 - \exp(-0.0714\,R_\delta)) \tag{21}$$

$$B_{1\theta} = \tau_u\, Pr_{t\infty} \tag{22}$$

$$f_{2\theta}\, B_{2\theta} = \tau_u \left(f_{2a\theta}\,\frac{2\,R}{R + C_\gamma} + f_{2b\theta}\sqrt{\frac{2\,R}{Pr}}\frac{1.3}{\sqrt{Pr}R_t^{3/4}}\right), \tag{23}$$

where $R_t = \kappa/(C_\mu \nu \omega)$ and $R_\delta = (d\sqrt{\kappa/R_t})/\nu$ with d the distance from the wall and $C_\gamma = 0.3$, $Pr_{t\infty} = 0.8$, $f_{2a\theta} = f_{1\theta}\exp(-4\times 10^{-6}\,R_t^2)$, $f_{2b\theta} = f_{1\theta}\exp(-2.5\times 10^{-5}\,{R_\delta}^2)$. There are three characteristic times in this modeling: the asymptotic dynamical time τ_u, the thermal time $\tau_\theta = R\,\tau_u$ and the mixed time τ_m, which is defined as $1/\tau_m =$

$1/\tau_u + 1/\tau_\theta = (R + C_\gamma)/(2\,\tau_u\,R)$. The dynamical time τ_u is simply proportional to the turbulent viscosity. Near the wall α_t/τ_u is proportional to $\sqrt{R}$ while in the asymptotic region α_t is independent of the time ratio. In the intermediate regions α_t/τ_u is proportional to $2\,R/(R + C_\gamma)$. The model functions f_j blend different behaviors in different regions. For details one can refer to [7, 8, 11, 12, 13, 14, 15] and references therein.

The average square temperature fluctuation κ_θ is obtained by the following transport equation [13]

$$\frac{\partial \kappa_\theta}{\partial t} + u_i \frac{\partial \kappa_\theta}{\partial x_i} = \frac{\partial}{\partial x_i}\left(\alpha + \frac{\alpha_t}{\sigma_{\kappa_\theta}}\right)\frac{\partial \kappa_\theta}{\partial x_i} + P_\theta - C_\mu \omega_\theta \kappa_\theta\,, \tag{24}$$

where

$$P_\theta = -\overline{u_i' T'}\,\frac{\partial T}{\partial x_i} = \alpha_t\,\frac{\partial T}{\partial x_i}\frac{\partial T}{\partial x_i}\,. \tag{25}$$

The equation for ω_θ is obtained from the one for ϵ_θ [3, 8, 13] with simple algebraic manipulations

$$\frac{\partial \omega_\theta}{\partial t} + u_i \frac{\partial \omega_\theta}{\partial x_i} = \frac{\partial}{\partial x_j}\left[\left(\alpha + \frac{\alpha_\theta}{\sigma_{\omega_\theta}}\right)\frac{\partial \omega_\theta}{\partial x_j}\right] + (C_{p1} - 1)\frac{P_\theta}{\kappa_\theta}\omega_\theta - (C_{d1} - 1)C_\mu \omega_\theta^2 + \\ + C_{p2}\frac{P_\kappa}{\kappa}\omega_\theta - C_{d2} C_\mu \omega \omega_\theta + \frac{2}{\kappa_\theta}\left(\alpha + \frac{\alpha_\theta}{\sigma_{\omega_\theta}}\right)\frac{\partial \kappa}{\partial x_j}\frac{\partial \omega_\theta}{\partial x_j}\,, \tag{26}$$

where P_κ is defined by (12) and P_θ by (25). For heavy liquid metals, with $Pr \approx 0.025$, we have used the coefficients $C_{d1} = 1.4$, $C_{p1} = 1.1$, $C_{d2} = 0.8$, $C_{p2} = 0.6$, $\sigma_{\kappa_\theta} = 1.4$ and $\sigma_{\omega_\theta} = 1.4$. If the system (24)-(26) is solved then the time ratio R can be computed directly as ω/ω_θ, the thermal eddy diffusivity can be computed as a function of the time ratio R and of the other time scales and the energy equation can be closed by substituting the turbulent heat flux.

Appropriate boundary conditions must be imposed in order to get a solution of the four parameter turbulence models defined above. We consider only near-wall approach and we check for each case that we have some mesh points with a non-dimensional distance from the wall $y^+ < 1$. This can be obtained by refining the mesh near the wall with a multigrid solver, as it is done in our code. We can enforce the boundary conditions on the wall as

$$\vec{u} = \vec{0}\,, \qquad \kappa = 0\,, \qquad \omega = \frac{6\nu}{C_\mu d^2}\,, \tag{27}$$

and for the thermal variables we impose constant heat flux on the wall. A more detailed discussion on boundary conditions to be used for the κ_θ-ω_θ system can be found in [3], in this work we impose the following boundary conditions for the thermal quantities:

$$\frac{\partial T}{\partial n} = -\frac{1}{\lambda}\,q_w\,, \qquad \kappa_\theta = 0\,, \qquad \omega_\theta = \frac{6\alpha}{C_\mu d^2}\,. \tag{28}$$

The time ratio R on the wall with these boundary conditions is set to the Prandtl number.

3 NUMERICAL RESULTS

In this section we report the numerical results obtained with the four parameter κ-ω-κ_θ-ω_θ turbulence model for fully developed turbulent flows in plane and cylindrical geometries. The Navier-Stokes system is solved by a fully coupled velocity-pressure solver implemented in an in-house finite element code. We use Taylor-Hood finite elements for Navier-Stokes system in order to satisfy the Inf-Sup condition and standard quadratic elements for temperature and κ-ω systems. In our code a multigrid solver is implemented, which allows multiple refinements of the grid to improve mesh resolution until the solution convergence has been reached. To use a near-wall approach for the turbulence model we need to have some mesh points in the viscous sublayer with $y^+ < 1$. For test cases with low velocity the coarse grid is usually sufficient to obtain this condition while for higher velocities we need to refine the grid until we satisfy the above condition. The numerical solution is checked by its L^2 norm. Let T_{h1} and T_{h2} be two different meshes over the domain Ω and u_{h_1} and u_{h_2} two corresponding solutions. The convergence criteria is set to

$$\frac{\|u_{h_{n-1}} - u_{h_n}\|_{L^2(\Omega)}}{\|u_{h_n}\|_{L^2(\Omega)}} \leq 10^{-4}, \tag{29}$$

where n is the refinement of the $n-1$ mesh discretization. The (29) assures full convergence for all the solutions. The physical properties of the liquid metal used in the simulations

Properties		**Values**	**Units**
Density	ρ	10340.	kg/m^3
Dynamic viscosity	μ	18.1×10^{-4}	$Pa \cdot s$
Thermal conductivity	λ	10.72	$W/(m \cdot K)$
Specific heat capacity	C_p	145.75	$J/(kg \cdot K)$

Table 1: Physical properties at the reference temperature.

are reported in Table 1. The Prandtl number of this fluid is very low, namely $Pr = 0.025$, so the thermal boundary layer develops deeply from the wall into the channel, while the dynamical boundary layer is much more thin. The molecular Prandtl number of 0.025 is a reference value for this class of fluids since mercury, lead an Lead-Bismuth-Eutectic (LBE) have a Prandtl number of $0.01 - 0.03$. The geometrical configurations we study are a plane channel with distance between the two plates $L = 0.0605$ m and with infinite dimension in the other directions and a cylindrical pipe with radius $r = 0.03025$. Since we want to study a fully developed flow we can make a change of variable in the energy solution. Indeed, in a fully developed flow with a constant heat flux on the wall, the bulk and the wall temperature are linear and the slope of the linear profile for unit of vertical length ΔT_b can be computed by writing an energy balance in the volume as

$$2\, L_x\, L_z\, q_w = C_p\, \dot{m} \Delta T_b\, L_x\ , \tag{30}$$

where the constant mass flow rate $\dot{m} = 2l\,\rho\,\bar{v}\,L_z$ appears. The steady energy equation can be written as

$$\frac{\partial}{\partial x_k}\,u_k\,T = \frac{\partial}{\partial x_k}\Big[(\alpha+\alpha_t)\frac{\partial}{\partial x_k}\,T\Big]\,, \tag{31}$$

together with appropriate boundary conditions. We may set

$$\frac{\partial T}{\partial n} = -\frac{1}{\lambda}q_w \qquad \text{on the wall}\,, \tag{32}$$

$$T = T|_i + L_x\,\Delta T_b \quad \text{in the outer section}\,, \tag{33}$$

where L_x is the axial length computational domain and $T|_i$ is the inlet temperature. This problem has not a unique solution since the integral form of (31), which is basically the (30), and (33) gives the condition (32) under fully developed flow hypotheses. The solution becomes unique if one fixes the average value of T or, equivalently, fixes the temperature in the first point of the wall [16]. In DNS computations the temperature is reported as a non-dimensional variable. In order to define this non dimensional temperature θ^+ one can expand the temperature solution T in the form

$$T = T_{w0} + x\,\Delta T_b - \theta\,, \tag{34}$$

where ΔT_b and T_{w0} are constant quantities and θ is the temperature distribution which is zero on the walls. After introducing (34) into (31) we obtain

$$\frac{\partial}{\partial x_k}\,u_k\,\theta = \frac{\partial}{\partial x_k}\Big[(\alpha+\alpha_t)\frac{\partial}{\partial x_k}\,\theta\Big] + \frac{v\,q_w}{l\,\rho\,C_p\,\langle v\rangle}\quad . \tag{35}$$

After solving the equation 35 one can normalize θ by dividing for the reference friction temperature defined as $T_\tau = q/(v_\tau \rho C_p)$ to obtain $\theta^+ = \theta/T_\tau$.

Test Case	Reynolds	Peclet
A	5500	140
B	13500	340
C	23700	600
D	39300	980
E	86500	2200
F	146000	3700
G	194000	4800
H	260000	6500
I	320000	8100

Table 2: Reynolds and Peclet numbers for plane geometry test cases.

In the following we report the numerical results obtained for the plane channel geometry described above with physical properties as reported in Table 1. Nine simulations have

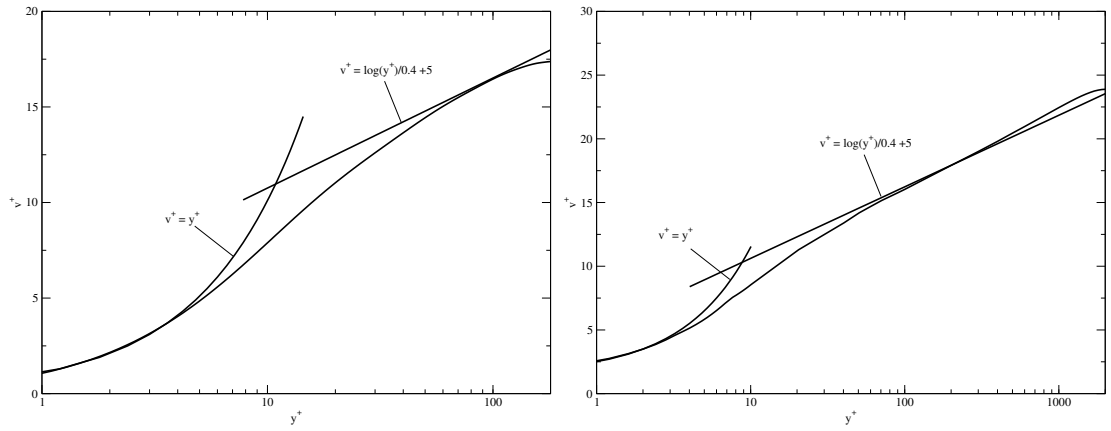

Figure 2: Non-dimensional velocity v^+ as a function of the non-dimensional distance from the wall y^+ for the test case A (left) and test case E (right).

been performed with Reynolds and Peclet numbers as reported in Table 2. The first two test correspond to a friction velocity base Reynolds number of $Re_\tau = 180$ and 395 and in the following we compare these results with DNS computations by Kawamura [9, 17, 18]. In Figure 2 the non-dimensional velocity v^+ normalized with the friction velocity v_τ is reported as a function of the non-dimensional distance from the wall y^+. On the left it is reported test case A with Reynolds number $Re \approx 5500$ while on the right test case E with $Re \approx 86500$. As one can see, the linear and logarithmic regions are well reproduced by κ-ω SST model. The comparison with DNS simulations is reported in Figure 3 on the left. Non-dimensional θ^+/Pr as a function of y^+ from DNS data for $Re_\tau = 180$ is reported with squares and labeled K180, while for $Re_\tau = 395$ it is shown with circles and labeled K395. The temperature profiles obtained with the four parameter model are reported with straight continuous lines and are compared with DNS data on the left. The non-dimensional temperature θ^+ is divided by the Prandtl number in order to better show the correct linear profile of the temperature near the wall. Both DNS data and our four parameter model correctly predict this linear behavior near the wall. Moreover DNS data are very similar to our numerical results for the two test cases compared. On the right one can appreciate the difference in slope of the θ^+ profile for test cases with higher velocities. The non-dimensional root-mean-square of the temperature fluctuation θ^+_{rms} as computed by the four parameter κ-ω-κ_θ-ω_θ turbulence model is reported in Figure 4 on the left as a function of y^+ for test cases A-G. It can be seen from this Figure that the thermal boundary layer is very deep inside the channel and that temperature fluctuations have a quite smooth profile. On the right of the same Figure it is reported the average turbulent Prandtl number as computed by the four parameter turbulence model. As one can see the Pr_t depends from the Peclet number and it decreases as the average velocity of the fluid increases. For the highest velocity test cases the Pr_t seems to reach a nearly constant value around 1.25.

The efficiency of the heat transfer from the heated solid wall to the liquid metal flow

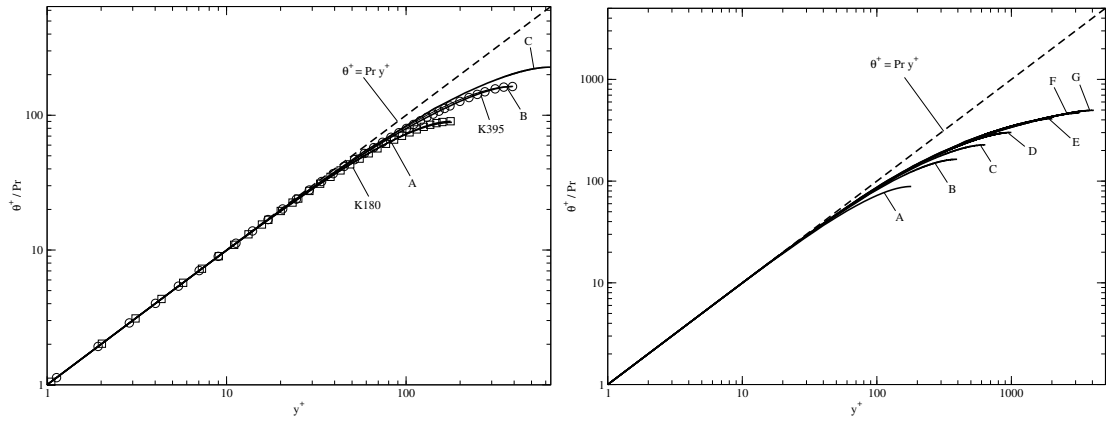

Figure 3: Non-dimensional temperature θ^+/Pr as a function of the non-dimensional distance from the wall y^+ for test cases *A*-*G* (right) computed with the four parameter model and compared with DNS data for $Re_\tau = 180$ (K180 square) and for $Re_\tau = 395$ (K395 circle) (left).

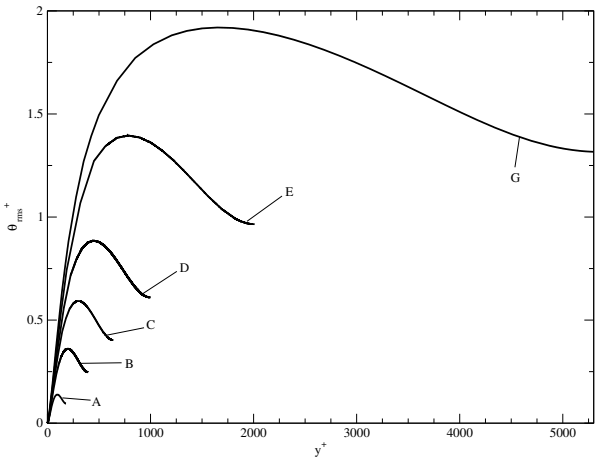

Pe	$\langle Pr_t \rangle$
140	2.28
340	2.08
600	1.94
980	1.79
2200	1.53
3700	1.37
4800	1.32
6500	1.27
8100	1.25

Figure 4: On the left non-dimensional root-mean-square temperature fluctuation θ^+_{rms} as a function of the non-dimensional distance from the wall y^+. On the right the table with average turbulent Prandtl number for all the studied test cases.

is described by the Nusselt number. For constant wall heat flux boundary conditions the Nusselt number is computed as

$$Nu = \frac{D_h \, q_w}{\lambda \Delta T} \, , \tag{36}$$

where D_h is the hydraulic diameter of the channel and ΔT is the difference between the wall temperature and the bulk temperature of the fluid. The asymptotic Nusselt number defines the heat removal of a liquid coolant from a heated wall, so it is the key quantity for practical heat transfer problems. Numerical results of the Nusselt number from the four parameter turbulence model are reported in Figure 5 on the left together with the DNS data for the first two test cases. As one can see the numerical results of the turbulence

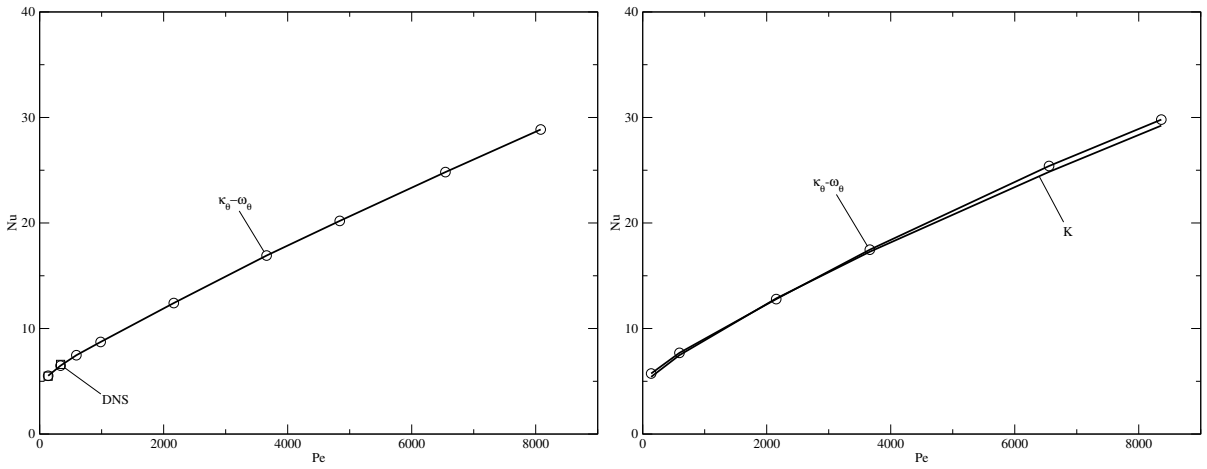

Figure 5: Asymptotic Nusselt number as a function of Peclet number. On the left plane channel geometry and numerical results from the four parameter turbulence model (circles) compared with DNS data (squares). On the right the numerical results of the four parameter turbulence model (circles) compared with the experimental Kirillov correlation (K) in cylindrical geometry.

model and the DNS data are quite similar.

We performed six simulations in cylindrical geometry with Peclet numbers in the range of 140 to 8400. The numerical results for velocity and temperature profiles are quite similar to those obtained in plane channel geometry, hence we do not show them here. We report only the results regarding the Nusselt number in order to compare the heat transfer predicted by the four parameter turbulence model with the one predicted by experimental heat transfer correlations which are available for this particular geometry. Liquid metal flows in cylindrical geometry have been studied experimentally more deeply because of the simple geometry and because these experimental results could be used for preliminary consideration on the heat transfer in more complex geometries, such as triangular or square rod bundles for advanced nuclear applications. A review of the experimental heat transfer correlations proposed by different authors can be found in [3]. In this paper we recall only Kirillov correlation (1) valid for liquid metal flows in cylindrical tube. In Figure 5 on the right the asymptotic Nusselt number computed with the four parameter turbulence model is compared with Kirillov experimental correlation for the heat transfer in this geometry. The match can be considered good for all considered Peclet numbers.

4 CONCLUSIONS

In this work we have tested the performance of a four parameter turbulence model for heavy liquid metal applications. This model is based on SST κ-ω model by Menter and on a thermal κ_θ-ω_θ turbulence model derived from the κ_θ-ϵ_θ model described in [3]. Two geometrical configurations have been studied, the plane channel flow and the cylindrical pipe flow, with a range of simulated Peclet numbers of approximately 150 to 8000. The

results obtained with the use of this model are encouraging because a good match is obtained with DNS data in plane geometry and Kirillov heat transfer correlation is quite well reproduced. The use of κ-ω models improves dramatically stability and robustness of the code and convergence is reached more easily with respect to the use of κ-ϵ systems, as previously done by the authors in [3, 4]. However more study is needed on this model to improve the heat transfer integral results and to obtain a more deep understanding of the physical phenomena involving turbulence modeling with a more accurate comparison with available DNS data.

ACKNOWLEDGMENTS

Financial support for this research was provided by EU project THINS (Thermal-hydraulics of Innovative Nuclear Systems) of the 7th Framework Programme.

REFERENCES

[1] X. Cheng and N. Tak, *Investigation on turbulent heat transfer to lead-bismuth eutectic flows in circular tubes for nuclear applications*, Nuclear Engineering and Design, Vol.236, pp. 385-393, 2006.

[2] X. Cheng and N.I. Tak, *CFD analysis of thermal-hydraulic behavior of heavy liquid metals in sub-channels*, Nuclear Engineering and Design, Vol. 236, pp. 1874-1885, 2006.

[3] F. Menghini and S. Manservisi, *A CFD Four Parameter Heat Transfer Turbulence Model for Engineering Applications in Heavy Liquid Metals* International Journal of Heat and Mass Transfer, Vol. 69, pp. 312-326, 2014.

[4] F. Menghini and S. Manservisi, *Triangular rod bundle simulations of a CFD κ-ϵ-κ_θ-ϵ_θ Heat Transfer Turbulence Model for Heavy Liquid Metals*, submitted to Nuclear Engineering and Design.

[5] P. Kirillov and P.A. Ushakov, *Heat transfer to liquid metals: specific features, methods of investigation, and main relationships*, Thermal Engineering, Vol. 48 (1), pp. 50-59, 2001.

[6] R. Z. Mehran and B. T. Farzad, *Implicit algebraic model for predicting turbulent heat flux in film cooling flow*, International Journal for Numerical Methods in Fluids, Vol.64, pp. 517-531, 2010.

[7] B. Deng, W. Wu and S. Xi, *A near-wall two-equation heat transfer model for wall turbulent flow*, International Journal of Heat and Mass Transfer, Vol.44, pp. 691-698, 2001.

[8] Y. Nagano and M. Shimada, *Development of a two equation heat transfer model based on direct simulations of turbulent flows with different Prandtl numbers*, Physics of Fluids, Vol.8, pp. 3379-3402, 1996.

[9] H Kawamura, H Abe and Y Matsuo, *DNS of turbulent heat transfer in channel flow with respect to Reynolds and Prandtl number effects.*, International Journal of Heat and Fluid Flow, Vol. 20, pp. 196-207, 1999.

[10] F.R. Menter, M. Kuntz and R. Langtry , *Ten Years of Industrial Experience with the SST Turbulence Model*, Turbulence, Heat and Mass Transfer 4, ed: K. Hanjalic, Y. Nagano, and M. Tummers, Begell House, Inc., , pp. 625-632, 2003.

[11] C.B. Hwang and C.A Lin, *A low Reynolds number two-equation $k_t - e_t$ model to predict thermal field*, International Journal of Heat and Mass Transfer, Vol. 42, pp. 3217-3230, 1999.

[12] K. Abe, T. Kondoh and Y. Nagano, *A new turbulence model for predicting fluid flow and heat transfer in separating and reattaching flows II. Thermal field calculations*, International Journal of Heat Mass Transfer, Vol.38(8), pp.1467-1481, 1995.

[13] H. Hattori, Y. Nagano and M. Tagawa, *Analysis of turbulent heat transfer under various thermal conditions with two-equation models*, Engineering Turbulence Modeling and Experiments 2 (Edited by W. Rodi and F. Martelli), pp. 43-52, 1993.

[14] Y. Nagano, C.Q. Pei and H. Hattori, *A New Low-Reynolds-Number One-Equation Model of Turbulence*, Flow, Turbulence and Combustion vol. 63, pp. 135151, 1999.

[15] K. Abe, T. Kondoh and Y. Nagano, *A two-equation heat transfer model reflecting second-moment closures for wall and free turbulent flows*, International Journal of Heat and Fluid Flow, Vol. 17, pp. 228-237, 1996.

[16] Piller, *Direct numerical simulation of turbulent forced convection in a pipe*, International Journal for Numerical Methods in Fluids 49, 583602, 2005.

[17] H Kawamura, K Osaka, H Abe and H Yamamoto, *DNS of turbulent heat transfer in channel flow with low to medium-high Prandtl number fluids.*, International Journal of Heat and Fluid Flow, Vol. 19, pp. 482-491, 1998

[18] H Kawamura, H Abe and Y Matsuo, *Surface heat-flux fluctuations in a turbulent channel flow up to $Re_\tau = 1020$ with $Pr = 0.025$ and 0.71.*, International Journal of Heat and Fluid Flow, Vol. 25, pp. 404-419, 2004.